PCCP

Spectroscopic mapping of the gold complex oligomers (dimer, trimer, tetramer, and pentamer) by excited-state coherent nuclear wavepacket motion in aqueous solutions

Journal:	*Physical Chemistry Chemical Physics*
Manuscript ID	CP-ART-10-2022-004823
Article Type:	Paper
Date Submitted by the Author:	15-Oct-2022
Complete List of Authors:	Iwamura, Munetaka; University of Toyama, Graduate School of Science and Engineering Urayama, Rina; University of Toyama, Graduate School of Science and Engineering Fukui, Airi; University of Toyama, Graduate School of Science and Engineering Nozaki, Koichi; University of Toyama, Graduate School of Science and Engineering Liu, Li; RIKEN, Molecular Spectroscopy Lab. Kuramochi, Hikaru; Institute for Molecular Science, Takeuchi, Satoshi; RIKEN Tahara, Tahei; RIKEN, Molecular Spectroscopy Lab

Spectroscopic mapping of the gold complex oligomers (dimer, trimer, tetramer, and pentamer) by excited-state coherent nuclear wavepacket motion in aqueous solutions

Munetaka Iwamura,[1]* Rina Urayama,[1] Airi Fukui,[1] Koichi Nozaki,[1] Li Liu[2,3], Hikaru Kuramochi,[2,3] Satoshi Takeuchi[2,3] and Tahei Tahara[2,3]*

[1]Graduate School of Science and Engineering, University of Toyama, 3190 Gofuku, Toyama 930-8555, Japan

[2]Molecular Spectroscopy Laboratory, RIKEN, 2-1 Hirosawa, Wako, Saitama 351-0198, Japan

[3]Ultrafast Spectroscopy Research Team, RIKEN Center for Advanced Photonics (RAP), RIKEN, 2-1 Hirosawa, Wako, Saitama 351-0198, Japan

Abstract

We investigate excited-state dynamics of the $[Au(CN)_2^-]$ oligomers following photo-initiated intermolecular Au-Au bond formation by carrying out femtosecond time-resolved absorption and emission measurements at various concentrations (0.080 – 0.6 mol/dm^3) with different photoexcitation wavelengths (290 – 340 nm). The temporal profiles of the time-resolved absorption signals exhibit clear oscillations arising from the Au-Au stretch coherent wavepacket motion of the excited-state oligomers, which is initiated with the photo-induced Au-Au bond formation. The frequency of the observed oscillation is changed with the change of the concentration, excitation wavelength, and wavelength of the excited-state absorption monitored, reflecting the change in the size of the oligomers detected. Fourier transforms (FTs) of the oscillations provide 2D plots of the FT amplitude against the oscillation frequency versus the detected wavelengths. Because the FT amplitude exhibits a node at the peak wavelength of the absorption of the species that gives rise to the oscillation, the 2D plots enabled us to determine the peak wavelength of the excited-state absorption of the dimer, trimer, tetramer, and pentamer. We also performed femtosecond time-resolved absorption measurements for the 0.3-mol/dm^3 solution with 260 nm photoexcitation, which is the condition employed in previous time-resolved X-ray studies (e.g., *Nature* 2015, 518 (7539)). It was found that various excited-state oligomers, including the dimer, were simultaneously generated under this condition, although the analysis of the previous time-resolved X-ray studies was made by assuming that only the excited-state trimer was generated. The obtained result means that the excited-state dynamics of the trimer claimed based on the time-resolved X-ray data is questionable and that re-analysis and re-examining of their data are necessary.

1. Introduction

$[Au(CN)_2^-]$ is one of the most primary and standard gold(I) complexes, and is known to form oligomers in aqueous solution due to the aurophilic interaction that is a weak attractive force working among the gold atoms.[1] The $[Au(CN)_2^-]$ oligomer attracts interest in the fields of coordination chemistry and photochemistry because these oligomers exhibit emission of various colors depending on the degree of the oligomerization that can be controlled by concentration and coexisting cations.[2-6] Recently, the $[Au(CN)_2^-]$ oligomer has also been recognized as an important system from the viewpoint of fundamental molecular science because it enables real-time observation of the bond formation dynamics. The lowest excited state of the $[Au(CN)_2^-]$ oligomer is characterized by the electronic excitation from an anti-bonding $d_z\sigma^*$ orbital to a bonding $p_z\sigma$ orbital among the gold atoms, and hence covalent bonds are formed among the gold complexes by the photoexcitation (Figure 1).[2, 3] Therefore, this system is suitable for studying ultrafast dynamics associated with the chemical bond formation, such as structural change of the resultant molecular assembly. From this viewpoint, ultrafast spectroscopic studies for $[Au(CN)_2^-]$ aqueous solutions have been carried out.[2, 3, 5, 7-14]

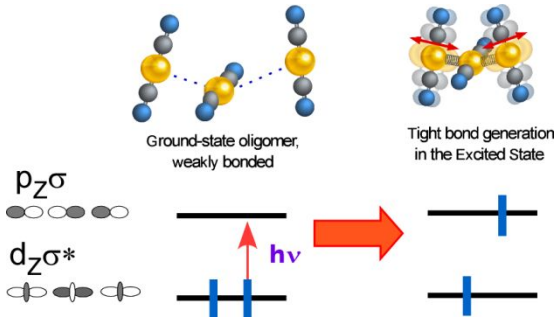

Figure 1. Ground state oligomer (trimer) and bond formation in the excited-state trimer.

The first study on the ultrafast dynamics of the $[Au(CN)_2^-]$ aqueous solution was carried out with femtosecond time-resolved absorption and emission spectroscopy, which we reported in 2013.[7] The experiment was performed by irradiation of 310-nm light to a 0.28-mol/dm^3 aqueous solution, intending to selectively photoexcite the trimer. In the obtained time-resolved absorption data, the oscillation due to the nuclear wavepacket motion was observed with a frequency of 85 cm^{-1}. Based on a quantum chemical calculation, this oscillation was attributed to the stretch vibration of the tight Au-Au bond in the trimer in the T_1 state, which experimentally confirmed the bond formation in the gold oligomers with photoexcitation. Furthermore, based on the fluorescence lifetime measurements and the temporal change of the excited-state absorption signals, it was concluded that the $S_1 \rightarrow T_1$ intersystem crossing and the bent-to-linear structural change in the excited-state trimer proceed

successively with the time constants of 0.5 ps and 2.1 ps, respectively.

Following this study, Kim et al. reported a time-resolved X-ray scattering study in 2015,[12] performed with short-wavelength pump pulses (267 nm) and a 0.3-mol/dm^3 solution. They analyzed the temporal profiles of the X-ray scattering signals containing information about the distance change among the Au atoms, and concluded that the bent-to-linear structural change was completed within 0.2 ps and then the Au-Au distance gradually shortened up to 1.6 ps. The time scale of the bent-to-linear structural change that they claimed (within 0.2 ps) was very different from the time constant determined by us (2.1 ps). Moreover, their argument of the 1.6-ps shortening of the Au-Au distance contradicts the 0.3-ps period of Au-Au stretch vibration (85 cm^{-1}) observed as the oscillation of the time-resolved absorption signal. Because the short-wavelength 267-nm pump light used in their experiments excited not only the trimers but also the dimers, it could be the origin of the controversy. Therefore, we performed the time-resolved absorption and emission measurements of a 0.038 mol/dm^3 aqueous solution with a pump light of 266 nm in 2016.[8] The obtained excited-state absorption spectra clearly showed spectroscopic evidence for the presence of the excited-state dimer, such as oscillation due to the Au-Au stretch motion of the dimer (130 cm^{-1}), and exhibited the excited-state dynamics of the dimer that is completely different from the trimer. On the other hand, the time-resolved X-ray group performed time-resolved X-ray scattering experiments using pump light of 310 nm and argued that the X-ray scattering signal at 0.2 ps after photoexcitation was the same as that obtained with excitation at 267-nm within the error.[13] They insisted that they observed only the excited-state trimer in their experiments regardless of the difference in the pump wavelength.

This controversy on the ultrafast dynamics of the [$Au(CN)_2^-$] trimer arises from the difficulty of distinguishing coexisting oligomers by time-resolved absorption spectroscopy or time-resolved X-ray scattering spectroscopy. Therefore, we applied ultrafast vibrational spectroscopy to this problem in 2019 and carried out time-resolved impulsive stimulated Raman spectroscopy (TR-ISRS) experiments.[10] Surprisingly, the obtained femtosecond time-resolved Raman spectra showed not only the excited-state trimer but also a noticeable amount of the excited-state tetramer even when a long wavelength (310 nm) pump light was used for irradiation of the 0.3 mol/dm^3 solution. Then, we performed TR-ISRS experiments on a solution with a lower concentration (0.1 mol/dm^3) using the 310-nm pump light to eliminate the contribution from the unwanted excited-tetramer and revealed the genuine photochemical dynamics of the trimer. Under this carefully set experimental condition, we obtained femtosecond time-resolved Raman spectra solely due to the excited-state trimer and observed that the Raman band attributed to the Au-Au stretch motion in the T_1 trimer shifts from 85 cm^{-1} to 92 cm^{-1} with a time constant of ~ 3 ps, which was attributed to the bent-to-linear structural change based on DFT calculations. The result of ultrafast vibrational spectroscopy clarified that the bent-to-linear structural change of the T_1 trimer proceeds on a time scale of several picoseconds, as

we claimed in our first paper.[7] After the TR-ISRS study, a new time-resolved X-ray scattering study that still used short-wavelength excitation at 270 nm was reported,[14] in which three nuclear wavepacket motions of 32, 79, and 125 cm^{-1} were observed through temporal oscillations of the X-ray scattering signal. They attributed the three vibrations to the T_1 trimer, but we note that the 130-cm^{-1} vibration arises from the *T_1 dimer* according to our previous analysis of the oscillatory component of femtosecond time-resolved absorption.[8]

As this history of the study on the ultrafast dynamics of the $[Au(CN)_2^-]$ trimer demonstrates, molecular vibration is a very sensitive structural marker for the excited-state oligomers of metal complexes: it is possible to distinguish oligomers of different sizes coexisting in the solutions based on the frequency of the metal-metal stretch vibration observed as the oscillation of the time-resolved absorption signals. Actually, we recently analyzed the oscillation of the time-resolved absorption signals of the metal complex oligomers using 2D plots for the oscillation frequency and detected wavelength (frequency–wavelength 2D plot),[9, 15] and successfully determined the peak wavelengths of the excited-state absorption band of excited-state oligomers of different sizes for the large excited-state $[Au(CN)_2^-]$ oligomers that were enhanced by the addition of tetraethylammonium chloride[9] as well as the excited-state $[Pt(CN)_4^{2-}]$ oligomers generated by photoexcitation.[15]

To disentangle the complex dynamics of each $[Au(CN)_2^-]$ oligomer having different sizes and ultimately settle down the controversy, it is desirable to systematically examine how the populations of excited-state oligomers with different sizes change with the change of the experimental conditions, i.e., concentrations and excitation wavelengths. Therefore, in this study, we systematically measure steady-state/time-resolved emission and absorption spectra of $[Au(CN)_2^-]$ aqueous solution at various concentrations and analyze the nuclear wavepacket motion observed as the oscillation of the time-resolved absorption signal using frequency–wavelength 2D plots. By integrating the information obtained with different spectroscopic approaches, the existence of excited-state oligomers from dimers to pentamers and their excited-state dynamics are clarified. We also perform femtosecond time-resolved absorption measurements using photoexcitation at 260 nm and the 0.3-mol/dm^3 solution to clarify the actual situation under the experimental condition adopted in the previous time-resolved X-ray scattering studies.[12, 14]

2. Results and Discussion

2.1. Femtosecond time-resolved absorption spectra

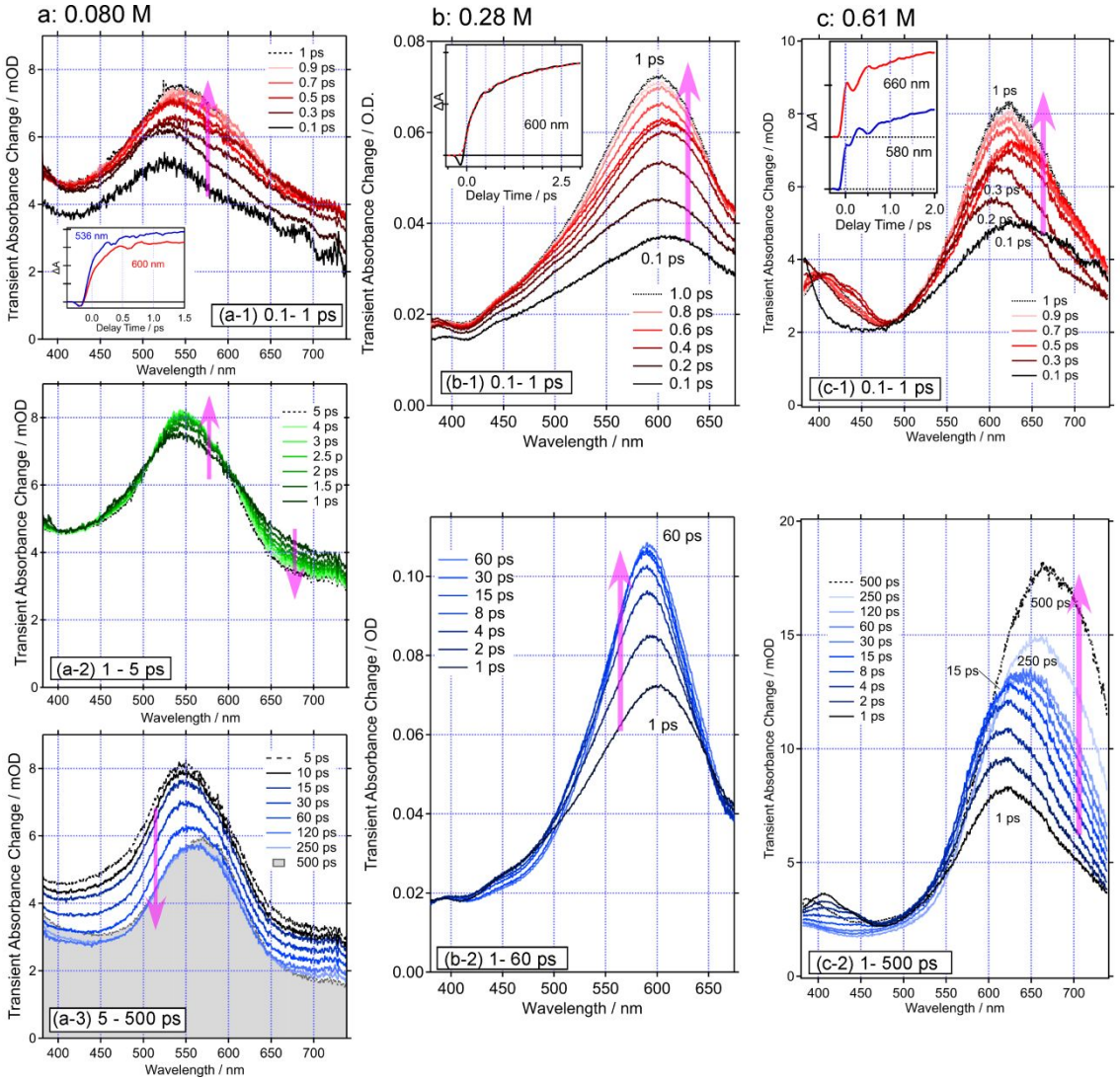

Figure 2. Time-resolved absorption spectra of $K[Au(CN)_2]$ aqueous solutions. (a) [Au] = 0.080 mol/dm^3, λ_{ex} = 290 nm for 0.1 – 1 ps (a-1), 1 – 5 ps (a-2) and 5 – 500 ps (a-3). (b) [Au] = 0.28 mol/dm^3, λ_{ex} = 310 nm for 0.1 – 1 ps (b-1) and 1 – 60 ps (b-2). (c) [Au] = 0.61 mol/dm^3, λ_{ex} = 340 nm for 0.1 – 1.0 ps (c-1) and 1 – 500 ps (c-2). Insets are temporal profiles of time-resolved absorption data at selected wavelengths. (Data in Figure 2b have been already reported in our previous paper[7].Reprinted with permission from *J. Am. Chem. Soc.*, 2013, 135, 538-541. Copyright [2013] American Chemical Society.)

Femtosecond time-resolved absorption spectra of $K[Au(CN)_2]$ aqueous solutions were measured at various concentrations, and the obtained spectra are shown in Figure 2. The three concentrations of 0.080, 0.28 and 0.61 mol/dm^3 were chosen to examine solutions that contain different populations of

the oligomers having different sizes, i.e., the dimer, trimer, tetramer, and larger oligomers. (The original data for the 0.28-mol/dm^3 solution has been already reported in our previous paper.[7]) The excitation wavelength was selected in the region of 260 – 340 nm to excite the red side of the absorption of each solution with different concentrations. These excitation conditions are favorable for exciting the largest oligomers that exist in each solution because the absorption extends to the longer wavelength side as larger oligomers are formed in the solution (Section S2 in Electronic Supplementary Information (ESI) for the detail).[7] In addition, these excitation conditions avoid excitation of the monomer because the monomer does not exhibit absorption in the wavelength region longer than 260 nm.[2, 7] Hereafter, we call these three experimental conditions Ex1, Ex2, and Ex3 (Ex1: [Au] = 0.080 mol/dm^3, λ_{ex} = 290 nm; Ex2: [Au] = 0.28 mol/dm^3, λ_{ex} = 310 nm; Ex3: [Au] = 0.61 mol/dm^3, λ_{ex} = 340 nm**)** for convenience. Picosecond time-resolved emission spectra were also measured with these three conditions to confirm the assignments of the excited-state species and to check the consistency with the steady-state emission spectra at various concentrations (Section S3 in ESI).

In all time-resolved absorption spectra obtained under Ex1, Ex2, and Ex3, the rise of the excited-state absorption band is commonly observed at around 500 – 700 nm in the femtosecond – early picosecond time region (Figure 2a-1, b-1, c-1). The intensity oscillations of the excited-state absorption band are also detected in this time region, which is more readily seen in the temporal profiles depicted in the insets of Figure 2a-1 b-1, c-1. After this rise, the time-resolved spectra taken under Ex1 (0.080 mol/dm^3, λ_{ex} = 290 nm) show a spectral change in the early picosecond time region and then exhibit decays with a time constant of 25 ps. This 25-ps decay of the excited-state absorption is attributable to the decay of the T_1 dimer because this time constant accords with the phosphorescence lifetime of the excited-state dimer (See ESI, section S3 or ref.[8]). We note that this 25-ps decay component is absent in the time-resolved spectra taken under Ex2 (0.28 mol/dm^3, λ_{ex} = 310 nm) and Ex3 (0.61 mol/dm^3, λ_{ex} = 340 nm), indicating that no noticeable excited-state dimers are generated under Ex2 and Ex3 that adopt longer-wavelength photoexcitations. This result is consistent with the conclusion of our previous study that no ground-state dimer absorption is present in the wavelength region longer than 300 nm.[7] Nevertheless, the time-resolved absorption spectra taken under Ex1 exhibit the excited-state absorption band peaked at 550 nm remains even after the T_1 dimer vanishes with a time constant of 25 ps (Figure 2-a3). This remaining excited-state absorption is highly likely assignable to excited-state trimer[8, 9] and indicates that the excited-state trimer is also generated even under Ex1.

In the time-resolved absorption spectra taken under Ex2 and Ex3, the excited-state absorption bands continue to rise on the picosecond time scale. Our previous study indicated that the rise of the time-resolved absorption on the picosecond time scale arises from the intersystem crossing and/or structural change of the oligomers larger than the dimer.[7-8] The rise of time-resolved absorption

observed under Ex2 is well reproduced by two time constants of 0.2 and 3 ps, while that measured with Ex3 is well fitted with two time constants of 1 and 10 ps (see ESI section S4 for the details). Moreover, the peak wavelength of the rising time-resolved absorption band observed under Ex2 (~590 nm) and Ex3 (~630 nm) is significantly different. This marked difference in time-resolved absorption spectra manifests that the excited-state oligomers with different sizes are generated and detected under Ex2 and Ex3. Because it is expected that larger oligomers are generated under Ex3 compared to Ex2, these data suggest that the excited states of larger oligomers exhibit absorption in a longer wavelength region and exhibit slower dynamics.

The time-resolved absorption spectra measured under Ex1, Ex2, and Ex3 look to be dominated by different but single bands. However, they contain contributions of different oligomers having different sizes. The coexistence of different excited-state oligomers is clearly shown by the analysis of the oscillatory component of the time-resolved absorption signals, as described in the next section.

2.2. Analysis of the oscillatory components

As already mentioned, clear oscillations are recognized in the temporal profiles of the time-resolved absorption signals measured under Ex1, Ex2, and Ex3 in the early delay time up to ~2 ps (Fig. 2a, b, and c). These oscillations reflect the excited-state nuclear wavepacket motions that are induced by the photoexcitation. To extract the oscillatory components and discuss them separately, we first carried out a global fitting analysis for the population component: We fitted multi-exponential functions to the temporal traces in the time region of 0 – 800 ps at selected ~40 wavelengths and determined 3 (for Ex 2) or 5 (for Ex 1 and Ex 3) common time constants. Then, with these common time constants, we fitted the population components of the temporal trace in the whole 0 – 2 ps time region at each wavelength (See Section S4 in ESI or our previous paper[7] for details). By subtracting the fitted population component from the temporal trances, we extracted oscillatory components. The obtained oscillatory components are shown in Figure 3a-1 (Ex1), 3b-1 (Ex2), and 3c-1 (Ex3), in the form of the monitored wavelength (horizontal axis) – delay time (vertical axis) 2D plot.

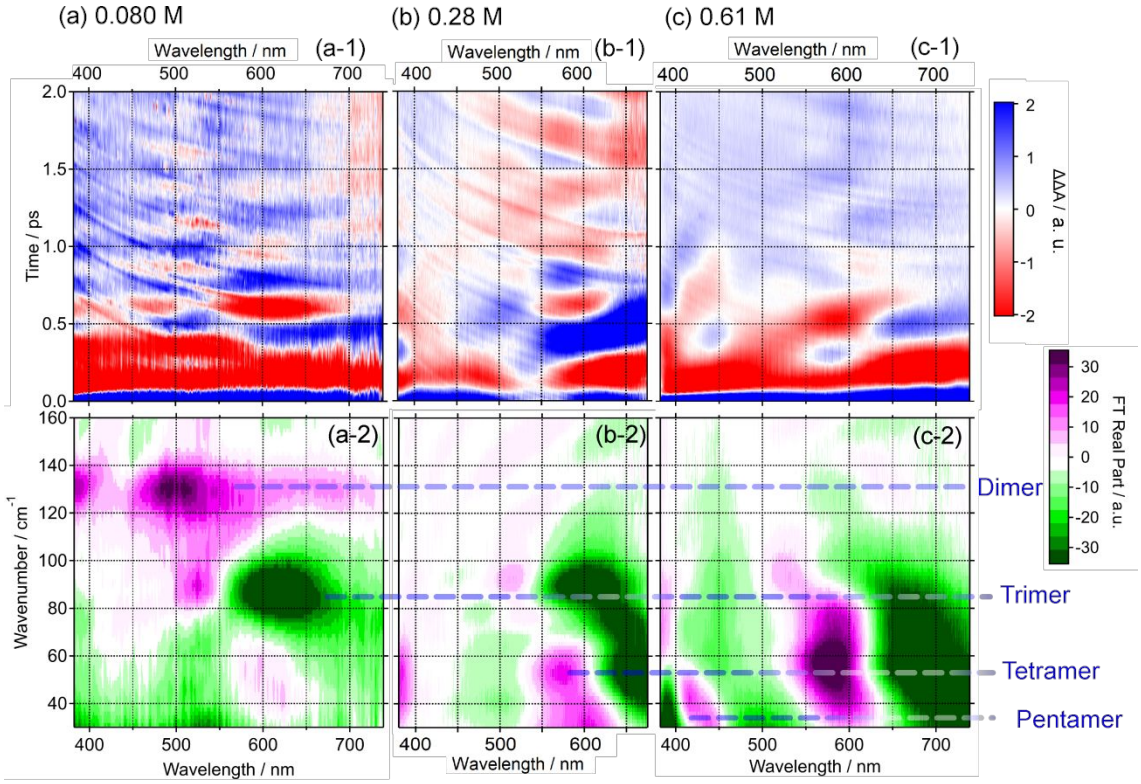

Figure 3. 2D plot for the oscillation of the femtosecond time-resolved absorption signal obtained from $K[Au(CN)_2]$ aqueous solution (a-1, b-1, c-1). Frequency–wavelength 2D plot of the real part amplitude of Fourier transform (a-2, b-2, c-2). (a: [Au] = 0.080 mol/dm^3, λ_{ex} = 290 nm; b: [Au] = 0.28 mol/dm^3, λ_{ex} = 310 nm; c: [Au] = 0.61 mol/dm^3, λ_{ex} = 340 nm. Original data in Figure 3b have already been reported in our previous paper.[7])

To analyze the observed oscillations, we performed FT analysis of the oscillatory components that are extracted from the data taken under Ex1, Ex2, and Ex3. Figure 3a-2, 3b-2, and 3c-2 show the amplitude of the real part of the calculated FT, which is plotted in the form of a frequency–wavelength 2D plot (See ESI Figure S9 for the 2D plots for the power and imaginary part amplitude.) The positive and negative values of the real parts are represented with purple and green, respectively.

As shown in Figure 3a-2, intense oscillations are seen at 130 cm^{-1} around 500 nm and 85 cm^{-1} around 525 and 640 nm under Ex1 (0.080 mol/dm^{-3} , λ_{ex} = 290 nm). This 130-cm^{-1} oscillation is not seen in the 2D plots obtained under Ex2 and Ex3. Because the excited-state dimer is generated only under Ex1 among the three conditions, the results indicate that the 130-cm^{-1} oscillation arises from the excited-state dimer. In particular, the 130-cm^{-1} oscillation, which remains up to several ps, is attributable to the 'T_1' dimer because the time-resolved absorption spectra obtained from a 0.038-mol/dm^{-3} solution with 266 nm excitation indicated that the $S_1 \rightarrow T_1$ intersystem crossing of the

dimer occurs with a time constant of ~0.2 ps.[8] The frequency of the oscillation of the T_1 dimer (129 cm^{-1}) observed in the previous study[8] also accords very well with the frequency detected in the present study. The previous study[8] showed that the T_1 dimer exhibits another totally symmetric Au-Au nuclear wavepacket motion with a frequency of 75 – 80 cm^{-1}. However, the corresponding peaks are hardly recognized in Figure 3a-2, although the existence of the T_1 dimer is strongly indicated by several experimental observations such as the 130-cm^{-1} oscillation, time-resolved emission spectra (Figure S3), and the ~25-ps decay of the excited-state absorption (Figure 3).

The 85-cm^{-1} oscillation at 525 nm (positive) and 640 nm (negative) are recognized in both Figure 3a-2 and Figure 3b-2. The same peaks are also recognized in Figure 3c-2, although the intensity is lower. Therefore, this oscillation is not assignable to the dimer because the excited-state dimer is not generated under Ex2 and Ex3. Hence, this vibration is assignable to the trimer. In fact, this 85-cm^{-1} oscillation has been assigned to the T_1 trimer in our previous time-resolved absorption and time-resolved impulsive stimulated Raman studies with help of quantum chemical calculations.[7-9]

The 55-cm^{-1} oscillation at 590 nm (positive) and at around 700 nm (negative) was commonly observed under Ex2 and Ex3 (Figure 3b-2 and c-2). The amplitude of this oscillation is larger than that of the 85-cm^{-1} oscillation of the T_1 trimer under Ex3 (0.61 mol/dm^3, λ_{ex}= 340 nm), while they are comparable under Ex2 (0.28 mol/dm^3, λ_{ex}= 310 nm). This indicates that the 55-cm^{-1} oscillation originates from an oligomer larger than the trimer, i.e., the tetramer. The excited-state tetramer in this time region is assignable to the S_1 state because its fluorescence lifetime of the tetramer is as long as 3 ps.[10]

The time-resolved absorption taken under Ex3 exhibits longer-wavelength excited-state absorption and slower dynamics than that under Ex2, indicating that excited-state larger oligomers are preferably generated under Ex3 compared to Ex2. Therefore, the oscillation even due to the pentamer is expected to appear in Figure 3c-2. Actually, the oscillatory components of ~40 cm^{-1} are recognized at 380 nm (negative), 420 nm (positive), ~600 nm (positive), and around ~700 nm (negative) in the 2D plot obtained under Ex3 (0.61-mod/dm^3, λ_{ex} = 340 nm; Figure 3c-2). Therefore, we assigned the 40-cm^{-1} oscillation to the pentamer (probably with some contribution of even larger oligomers). The 40-cm^{-1} oscillations at ~600 and ~700 nm with opposite phases were also observed in the solution containing tetraethylammonium chloride, which has been attributed to the excited-state pentamer.[9] This excited state of the pentamer is the S_1 state because the lifetime of the fluorescence component that is seen under Ex3 is longer than ~ 10 ps. (See ESI, Section S3)

It is worth noting that several pairs of positive and negative amplitudes are observed at the common frequency in the 2D plots. For example, the vibrational peaks of the T_1 trimer (85 cm^{-1}) and S_1 tetramer (55 cm^{-1}) show negative and positive pairs of the vibrational peaks as mentioned above. The vibration of the pentamer (40 cm^{-1}) also exhibits this characteristic, although the peak positions at ~600 and ~700 nm are somewhat unclear. With the typical Franck-Condon mechanism, a totally

symmetric nuclear wavepacket motion induces frequency oscillation of the absorption band, giving rise to the modulation of absorption intensity at the short and long-wavelength side of the absorption maximum with opposite phases[16] (Figure 4). Thus, the appearance of such an oscillation pair of the opposite phases is a signature of a totally symmetric nuclear motion, and it provides information about the peak wavelength of the oscillating excited-state absorption band. The node of 85-cm^{-1} vibration is located at 550 nm, indicating that the absorption maximum of the T_1 trimer is located at 550 nm. The 55-cm^{-1} vibration has a node at 620 nm, indicating that the S_1 tetramer exhibits an absorption maximum at 620 nm. The S_1 pentamer has absorption peaked at 400 nm and ~640 nm because the nodes are recognized at these wavelengths. The 400-nm absorption peak is clearly seen in the absorption spectra taken under Ex3 in the time region earlier than 1 ps (Figure 2c-1), whereas the ~640-nm absorption is recognized but the peak position is unclear due to the overlap of the absorption bands in the spectra. It is noted that a positive FT peak of the 130-cm^{-1} vibration for the T_1 dimer was seen at 500 nm in the 2D plot, but the corresponding negative peak is absent. It may suggest that the negative peak is located in the shorter wavelength region that is out of the observed wavelength range.

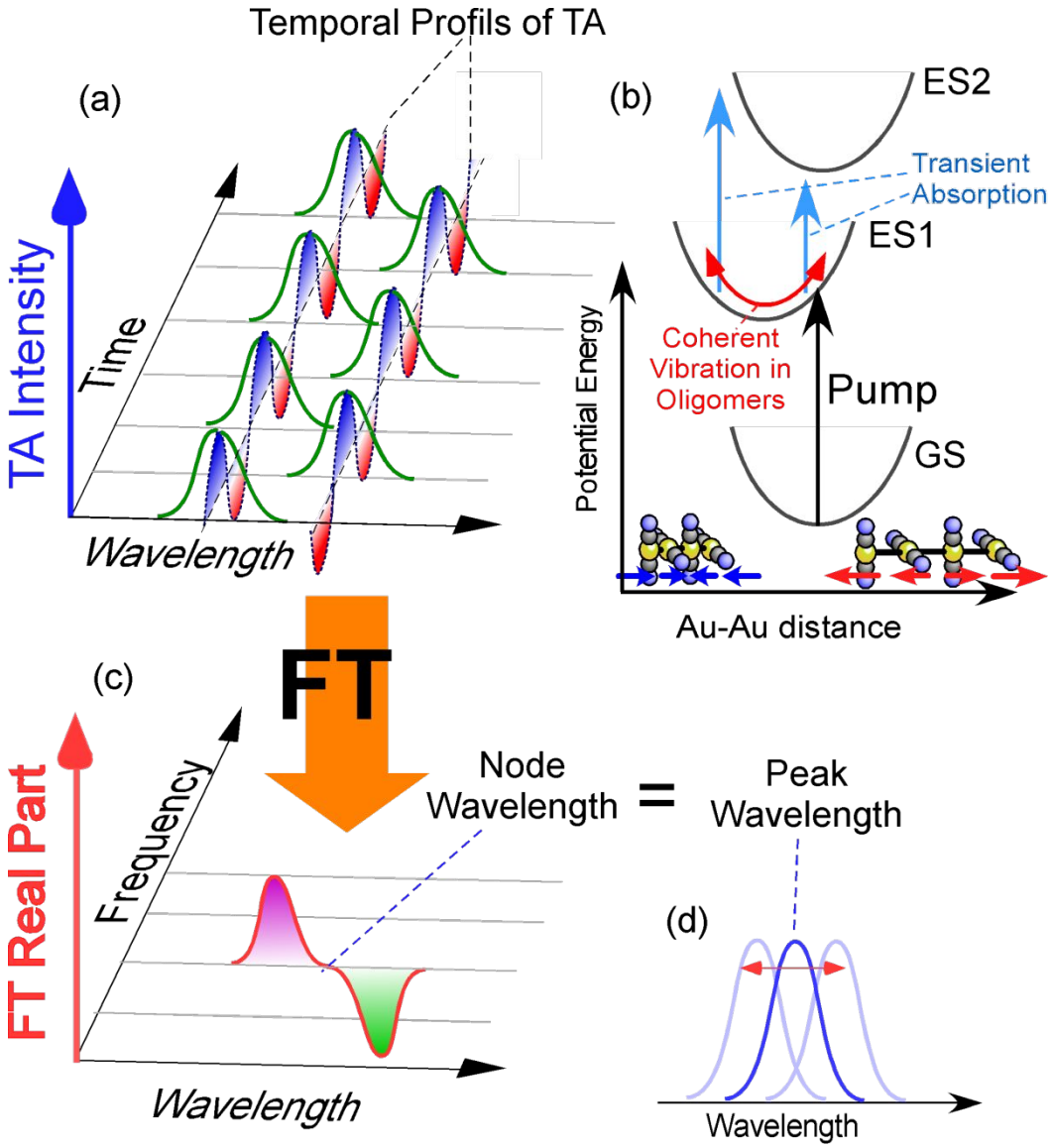

Figure 4. Schematic illustrations for the oscillation of the excited-state absorption based on the Franck-Condon mechanism. (a) Time-resolved absorption band showing the temporal oscillation of the peak wavelength due to the nuclear wavepacket motion and their temporal profiles. (b) Potential energy surfaces along the Au-Au stretch coordinate of an oligomer in the ground state (GS) and excited states (ES1 & ES2). (c) Vibrational spectrum obtained as the real part of Fourier transform of the oscillatory component in the time-resolved absorption data. (d) Excited-state absorption of the ES1 state at the equilibrium state (dark blue) and vibrationally coherent state (pale blue).

The analysis of the frequency–wavelength 2D plot succeeded in identifying excited-state T_1 dimer (130 cm^{-1}), T_1 trimer (85 cm^{-1}), S_1 tetramer (55 cm^{-1}), and S_1 pentamer (~ 40 cm^{-1}) based on their nuclear wavepacket motions. The peak wavelengths of the corresponding excited-state absorption

bands are also determined to be 550 nm for T_1 trimer, 620 nm for S_1 tetramer, and 400 and ~660 nm for S_1 pentamer from the node of the amplitude of the corresponding oscillations.

2.3. Time constants of spectral changes and their assignments

As described in section 2.2, the fitting analysis for the population components in the temporal profiles of the time-resolved absorption signals provided characteristic time constants of the spectral changes observed under the three experimental conditions (Ex1–3). Because the excited-state oligomers generated under the three conditions have been identified by the analysis of the excited-state coherent nuclear wavepacket motion in the previous section, we can make assignments of these time constants to the relevant dynamics of the excited-state oligomers with different sizes, i.e., from the dimer to the pentamer.

The time constants observed under Ex1 are 0.2, 2 and 25 ps. Among them, 25 ps is assignable to the lifetime of the T_1 dimer, as already mentioned. The time constant of the $S_1 \rightarrow T_1$ intersystem crossing of the dimer was reported to be 0.2 ps from femtosecond time-resolved absorption,[8] and the bend-to-linear structural change in the T_1 trimer has been determined to be 2 ps based on the vibrational frequency change observed by TR-ISRS.[10] Therefore, 0.2 and 2 ps are assignable to the intersystem crossing of the dimer and structural change in the trimer, respectively. In addition, the 0.2-ps component highly likely includes the contribution from the intersystem crossing of the trimer because this time constant is close to the intersystem crossing time of the trimer (0.38 ps), which was determined from the fluorescence lifetime.[7, 10] These characteristic time constants imply that both of the excite-state dimer and excited-state trimer are generated and detected under Ex1.

The time constants obtained from the data measured under Ex2 are 0.3 and 2 ps. The excited-state species generated under Ex2 are the trimer and the tetramer, and the time constants of their $S_1 \rightarrow T_1$ intersystem crossing have been reported to be 0.38 and 2.6 ps, respectively.[7, 10] Therefore, 0.3 ps and 2 ps are assignable to the intersystem crossing of the trimer and the tetramer, respectively. We note that the time constant of the structural change of the T_1 trimer is 2 ps[10], so the 2-ps spectral change also includes that due to the structural change of the T_1 trimer.

The time constants obtained under Ex3 are 1 and 10 ps. Because the excited-state species generated under Ex3 are the tetramer and pentamer, these time constants are assignable to their dynamics. The 1-ps process is assignable to the intersystem crossing of the tetramer because it is close to the fluorescence lifetime of the tetramer (2.6 ps).[10] The 10-ps process is assignable to the $S_1 \rightarrow T_1$ intersystem crossing of the pentamer because the fluorescence decay observed under Ex3 includes a 10-ps component (See ESI, section S3).

The frequency of the excited-state coherent nuclear motion, excited-state absorption peak wavelength, and time constants of the intersystem crossing of the $[Au(CN)_2^-]$ oligomers with

different sizes are summarized in Table 1. In addition, the information about their T_1 states is also listed in the table: The T_1 lifetimes were determined from the phosphorescence lifetimes measured in the present study (See ESI section S3) and/or previous studies.[5, 8] The phosphorescence bands of $K[Au(CN)_2]$ aqueous solutions are peaked at 390, 430, and 460 nm, and their lifetimes are 1.4 ns (trimer), 23 ns (tetramer), and 15 ns (pentamer), respectively (See ESI Section S3 and literature[5, 8]).

Table 1. Characteristic properties of the excited-state $[Au(CN)_2^-]_n$ oligomers with different sizes. The frequencies of coherent Au-Au stretch motions (ν), the peak wavelengths of the excited-state absorption (λ_{Abs}), the peak wavelengths and the lifetimes of the fluorescence (λ_F and τ_F) and those of phosphorescence (λ_P and τ_p). Note that τ_F corresponds to the intersystem crossing time from S_1 to T_1.

Oligomers	ν / cm^{-1} (States)	$\lambda_{Abs.}$ / nm (States)	λ_F / nm	τ_F / ps	λ_P / nm	τ_p / ns
dimer	130 (T_1)	-	-	-	330	0.025
trimer	90 (T_1)	550 (T_1)	350	0.38[a]	390	1.4
tetramer	55 (S_1)	620 (S_1)	~380	2.6[a]	430	23[b]
pentamer	≤40 (S_1)	400, ~660 (S_1)	~430	13	460	15[b]

a) SI in Ref. 10 b) Ref. 5

2.4. Re-examination of the origin of the controversy

As we described in the introduction, there is a controversy about the time constants of the excited-state structural change in the trimer between the time-resolved X-ray studies (< 0.2 ps)[12] and our time-resolved absorption/Raman studies (2 ps)[7, 10]. This disagreement arises from the difference in the treatment of the equilibrium among the oligomers in the analysis. In particular, the X-ray groups analyzed their data by assuming that only the excited-state trimer was present in the solution of their experiments carried out for a ~0.30 mol/dm^3 solution with ~270 nm excitation.[12, 14, 17] However, our studies clearly showed that various sizes of the excited-state oligomers, i.e., the dimer, trimer and tetramer in the excited state, are generated, depending on the concentration and excitation wavelength. To clarify the actual situation under the experimental condition of the previous X-ray experiments, we performed femtosecond time-resolved absorption measurements for 0.30 mol/dm^3 $[Au(CN)_2^-]$ aqueous solutions using 260-nm excitation.

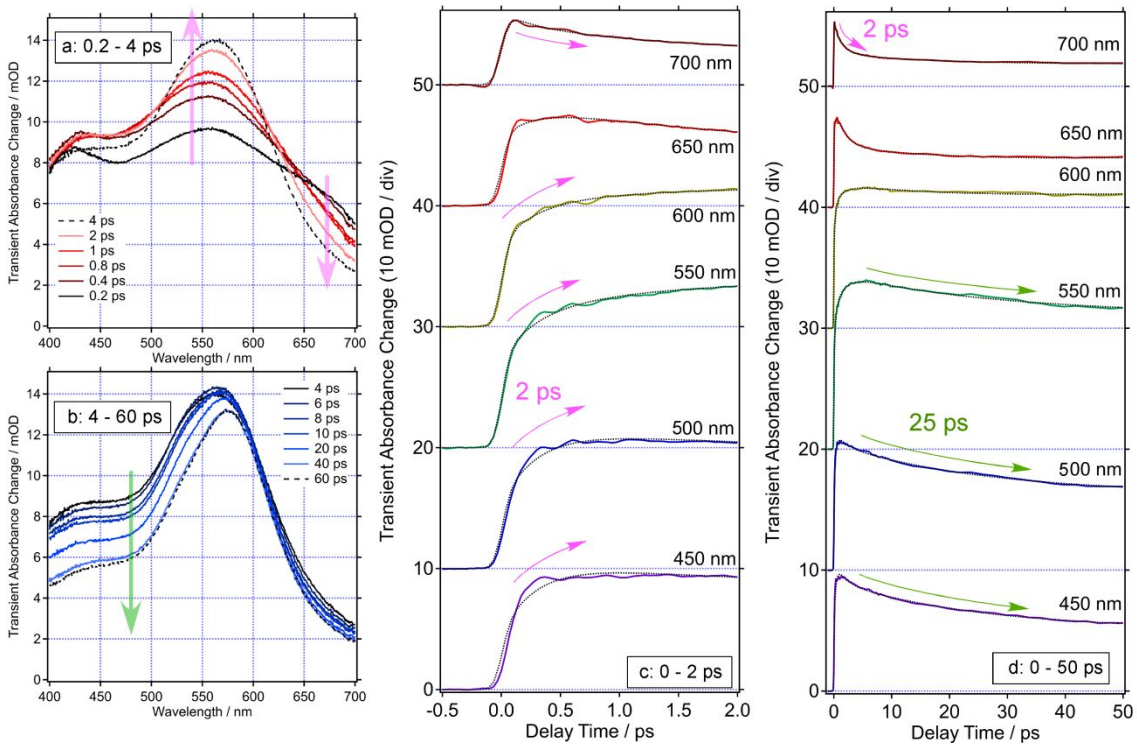

Figure 5. Time-resolved absorption data of the $K[Au(CN)_2]$ aqueous solution ([Au] = 0.30 mol/dm^3, λ_{ex} = 260 nm). Time-resolved absorption spectra in the time regions of 0.2 – 4 ps (a), 4 – 60 ps (b). Temporal profiles of time-resolved absorption at selected wavelengths in the time regions of 0 – 2 ps (c) and 0 – 50 ps (d).

The obtained femtosecond time-resolved absorption data are shown in Figures 5 and 6. As seen in Figure 5, the spectral change in the delay time region up to ~60 ps are dominated by a ~2-ps rise at around 550 nm and a ~25-ps decay in the 400 – 600 nm wavelength region. These spectral changes are very similar to those observed in the time-resolved absorption spectra taken under Ex1. In particular, the distinct ~ 25-ps decay, which is seen in the 400 – 600 nm region, is very similar to the spectral change due to the decay of the T_1 dimer (Figure 3). It strongly indicates that the excited-state dimer is generated under this experimental condition.

Oscillations of the time-resolved absorption signal were also observed in the early time region, as shown in Figure 6-a. The corresponding frequency–wavelength 2D plot is shown in Figure 6-b. (See ESI Figure S10 for the 2D plots for the power and imaginary part amplitude.) Various coherent nuclear motions are recognized in the frequency region of 30 – 140 cm^{-1} and the wavelength region of 400 – 700 nm, suggesting that various excited-state species are simultaneously generated. Some peaks of the oscillation amplitudes are unclear in the 2D plot, which may be due to the overlap and interference among various oscillatory signals that appear close to each other. Nevertheless, we can clearly recognize distinct peaks at 130 and 60 cm^{-1} (Figure 6-b). The detected wavelengths where the 130-cm^{-1} oscillations appear are similar to those in Figure 3, confirming that the T_1 dimer is generated under this experimental condition. On the other hand, the wavelengths where the most

distinct oscillation at 60 cm^{-1} appears (430 and 530 nm, Figure 6-b) are different from that of the 55-cm^{-1} oscillation observed under Ex2 and Ex3 (590 nm and 700 nm, Figure 3). This implies that excited-state species giving the 60-cm^{-1} oscillation in the 400 – 500 nm region are different from those observed under Ex2 and Ex3. The unknown excited-state species should be oligomers because there is no absorption of the ground-state monomer at 260 nm, so the excited-state monomer cannot be generated. Probably, they are excited-state oligomers that have structures substantially different from stable structures (typically, the stable excited-state structure is linear-staggered structures),[3, 7] such as heavily bent and/or zig-zag oligomers, which cannot be generated by the long wavelength photoexcitation but can be produced only by the short wavelength excitation. Anyway, the results of this measurement demonstrate that the 260-nm excitation generates excited-state dimer and other unknown excited-state species. This implies that the assumption of the previous X-ray studies is not adequate and hence that re-analysis or re-investigation is needed for the time-resolved X-ray scattering data recorded with excitation at ~260 nm.[12, 14]

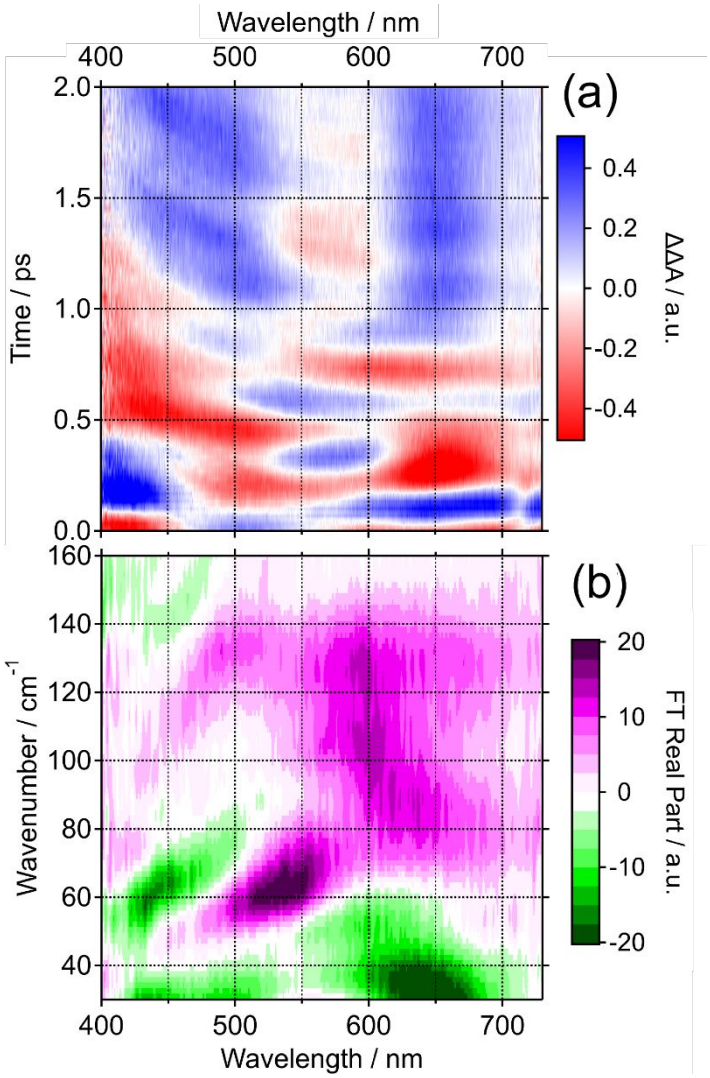

Figure 6. 2D plot for the oscillation of the femtosecond time-resolved absorption signal from $K[Au(CN)_2]$ aqueous solution (a). Frequency–wavelength 2D plot of the real part amplitude of the Fourier transform (b) ([Au] = 0.30 mol/dm^3, λ_{ex} = 260 nm)

3. Summary

We measured and analyzed femtosecond time-resolved absorption spectra of pure $K[Au(CN)_2]$ aqueous solutions of various concentrations, and made solid assignments of the peak wavelengths of excited-state absorption and frequencies of excited-state coherent nuclear motion of the oligomers having different sizes (from dimer to pentamer). It was revealed that the excited-state oligomers with different sizes are generated in the solutions and that the excited-state species detected are very dependent on the concentration and excitation wavelengths. In particular, the excited-state species generated by ~260 nm photoexcitation of the 0.3 mol/dm^3 solution is not dominated by the trimer,

but other oligomers such as dimer and other unknown species are generated. We stress that spectroscopic information obtained with systematically changing concentration and excitation wavelength is critically important for elucidating the excited-state dynamics of the oligomers of metal complexes in the solution.

The analysis of the coherent nuclear wavepacket motion observed in the time domain, which was employed in this work, is very powerful for elucidating excited-state species with their absorption peak wavelengths for the systems that simultaneously contain multiple metallophilic oligomers in the excited state. These days, various systems of new metallophilic oligomers with their attractive spectroscopic properties have been found.[6, 18-22] We think that further investigation of these metallophilic systems using the analysis of the coherent nuclear wavepacket motion is very promising for revealing their unique photochemical properties.[9, 15]

Acknowledgements

This work was supported by KAKENHI (15K05447 and 20K05526), and JST, PRESTO Grant Number JPMJPR17P4, Japan.

Electronic Supplementary information available

Following contents are given in Supporting Information. S1. Experimental Section; S2. Concentration dependence of the steady-state absorption spectra; S3. Steady-state and picosecond time-resolved emission spectra; S4. Femtosecond time-resolved absorption; S5. Time-resolved absorption spectra of $K[Au(CN)_2]$ aqueous solution of 0.30 mol/dm^3, λ_{ex} = 260 nm.

Conflicts of interest

There are no conflicts to declare.

References

1. H. H. Patterson, S. M. Kanan and M. A. Omary, *Coord. Chem. Rev.*, 2000, **208**, 227-241.
2. M. A. Rawashdeh-Omary, M. A. Omary and H. H. Patterson, *J. Am. Chem. Soc.*, 2000, **122**, 10371-10380.
3. M. A. Rawashdeh-Omary, M. A. Omary, H. H. Patterson and J. John P. Fackler, *J. Am. Chem. Soc.*, 2001, **123**, 11237-11247.
4. Z. Guo, R. L. Yson and H. H. Patterson, *Chem. Phys. Lett.*, 2007, **433**, 373-378.
5. R. Wakabayashi, J. Maeba, K. Nozaki and M. Iwamura, *Inorg. Chem.*, 2016, **55**, 7739-7746.
6. H. Schmidbaur and H. G. Raubenheimer, *Angew. Chem. Int. Ed.*, 2020, **59**, 14748-14771.
7. M. Iwamura, K. Nozaki, S. Takeuchi and T. Tahara, *J. Am. Chem. Soc.*, 2013, **135**, 538-541.

8. M. Iwamura, R. Wakabayashi, J. Maeba, K. Nozaki, S. Takeuchi and T. Tahara, *Phys. Chem. Chem. Phys.*, 2016, **18**, 5103-5107.
9. M. Iwamura, K. Kimoto, K. Nozaki, H. Kuramochi, S. Takeuchi and T. Tahara, *J. Phys. Chem. Lett.*, 2018, **9**, 7085-7089.
10. H. Kuramochi, S. Takeuchi, M. Iwamura, K. Nozaki and T. Tahara, *J. Am. Chem. Soc.*, 2019, **141**, 19296-19303.
11. S. H. Sohn, W. Heo, C. Lee, J. Kim and T. Joo, *J. Phys. Chem. A*, 2019.
12. K. H. Kim, J. G. Kim, S. Nozawa, T. Sato, K. Y. Oang, T. W. Kim, H. Ki, J. Jo, S. Park, C. Song, T. Sato, K. Ogawa, T. Togashi, K. Tono, M. Yabashi, T. Ishikawa, J. Kim, R. Ryoo, J. Kim, H. Ihee and S.-i. Adachi, *Nature*, 2015, **518**, 385-389.
13. K. H. Kim, J. G. Kim, K. Y. Oang, T. W. Kim, H. Ki, J. Jo, J. Kim, T. Sato, S. Nozawa and S.-i. Adachi, *Struct. Dyn.*, 2016, **3**, 043209.
14. J. G. Kim, S. Nozawa, H. Kim, E. H. Choi, T. Sato, T. W. Kim, K. H. Kim, H. Ki, J. Kim and M. Choi, *Nature*, 2020, **582**, 520-524.
15. M. Iwamura, A. Fukui, K. Nozaki, H. Kuramochi, S. Takeuchi and T. Tahara, *Angew. Chem. Int. Ed.*, 2020.
16. K. Ishii, S. Takeuchi and T. Tahara, *J. Phys. Chem. A*, 2008, **112**, 2219-2227.
17. S. H. Sohn, W. Heo, C. Lee, J. Kim and T. Joo, *J. Phys. Chem. A*, 2019, **123**, 6904-6910.
18. H. Schmidbaur and A. Schier, *Chem. Soc. Rev.*, 2008, **37**, 1931-1951.
19. V. V. Sivchik, E. V. Grachova, A. S. Melnikov, S. N. Smirnov, A. Y. Ivanov, P. Hirva, S. P. Tunik and I. O. Koshevoy, *Inorg. Chem.*, 2016, **55**, 3351-3363.
20. V. W.-W. Yam and E. C.-C. Cheng, *Chem.Soc.y Rev.*, 2008, **37**, 1806-1813.
21. A. Ito, M. Iwamura and E. Sakuda, *Coord. Chem. Rev.*, 2022, **467**, 214610.
22. A. Aliprandi, D. Genovese, M. Mauro and L. De Cola, *Chem. Lett.*, 2015, **44**, 1152-1169.